Check for updates

Synergistic regulation of Notch signaling by different O-glycans promotes hematopoiesis

Ankit Tanwar and Pamela Stanley*

Department of Cell Biology, Albert Einstein College of Medicine, New York, NY, United States

Glycosylation of Notch receptors by O-fucose glycans regulates Notch ligand binding and Notch signaling during hematopoiesis. However, roles in hematopoiesis for other O-glycans that modify Notch receptors have not been determined. Here we show that the EGF domain specific GlcNAc transferase EOGT is required in mice for the optimal production of lymphoid and myeloid cells. The phenotype of *Eogt* null mice was largely cell-autonomous, and Notch target gene expression was reduced in T cell progenitors. Moreover, EOGT supported residual Notch signaling following conditional deletion of *Pofut1* in hematopoietic stem cells (HSC). *Eogt : Pofut1* double mutant HSC had more severe defects in bone marrow and in T and B cell development in thymus and spleen, compared to deletion of *Pofut1* alone. The combined results show that EOGT and O-GlcNAc glycans are required for optimal hematopoiesis and T and B cell development, and that they act synergistically with POFUT1 and O-fucose glycans to promote Notch signaling in lymphoid and myeloid differentiation.

KEYWORDS

Notch signaling, O-glycans, HSC, lymphoid, myeloid

Highlights

- O-GlcNAc glycans and EOGT promote lymphopoiesis and myelopoiesis.
- EOGT supports Notch signaling in the absence of POFUT1 and O-fucose glycans.

Introduction

Notch signaling is highly conserved and plays crucial roles in cell fate determination and tissue development (1). There are four Notch receptors (NOTCH1 to NOTCH4) that can be activated by canonical Notch ligands (DLL1, DLL3, DLL4, JAG1 and JAG2) to induce Notch signaling in mammals. Notch ligand binding and Notch signaling are regulated by glycosylation of the extracellular domain (ECD) of Notch receptors (2, 3).

Structural studies reveal direct interactions between Notch ligands and O-fucose in specific epidermal growth factor-like (EGF) repeats of NOTCH1 (4, 5). Following Notch ligand engagement, an ADAM metalloprotease cleaves NECD, followed by a second cleavage by the γ-secretase complex. Notch intracellular domain (NICD) complexes in the nucleus with the transcriptional repressor RBP-Jk, and co-activators including Mastermind-like-1 (MAML1), to induce the expression of Notch target genes, including Hairy enhancer-of-split (Hes) and Hairy-related gene families, which regulate the expression of many other genes (6, 7).

Within the hematopoietic system, Notch signaling plays important roles in regulating different stages of lymphoid and myeloid development (8, 9). DLL4-induced NOTCH1 signaling is indispensable for T cell development in the thymus. Thus, conditional inactivation of Notch1 or Dll4 using Mx1-Cre is sufficient to block T cell development (10, 11). However, Notch2 is also required for optimal development of early T cell progenitors (12). DLL1-induced NOTCH2 signaling is essential for the generation of marginal zone B cells (MZ-B) in the spleen (13, 14). O-fucose glycans extended by LFNG and MFNG promote the formation of MZ-B cells (15) and all three FNG genes contribute to T and B cell development (16).

Consensus sites within EGF repeats in the NECD of Notch receptors carry O-fucose, O-glucose and O-GlcNAc glycans (17) (Figure 1). EGF repeats with appropriate consensus sites occur in ~50 proteins of the proteome, including Notch receptors and Notch ligands (19, 20). O-fucose is transferred by protein O-fucosyltransferase 1 (POFUT1), which is further extended by the Fringe family of glycosyltransferases (LFNG, MFNG and RFNG). Misexpression of Lfng in thymus disrupts T cell development (21–23). Conditional deletion of Pofut1 in the bone marrow leads to the disruption of hematopoiesis with an increase in granulocyte-monocyte progenitors (GMP), and a reduction in common myeloid progenitors (CMP) (24). This causes a block in T cell production in thymus and MZ-B cell production in spleen, accompanied by an increase in granulocytes in spleen. Notch

FIGURE 1

Expression of *Eogt* and *Pofut1* in immune cell subsets. The diagram depicts the ECD of mouse NOTCH1 showing the O-glycans attached at respective consensus sites in the 36 EGF repeats. The sugar that initiates each O-glycan is shown in the key. The potential sugar extensions from O-fucose and O-GlcNAc glycans are also shown. The expression of *Eogt* and *Pofut1* in a number of immune cells is taken from ImmGen Gene Skyline ULI RNASeq data group for *Eogt* and *Pofut1* gene expression (18) (http://rstats.immgen.org/Skyline/skyline.html). The definition of each immune cell type is given at the link. Expression of *Eogt* and *Pofut1* vary inversely in certain immune cell subsets.

ligand binding and Notch signaling are markedly reduced in hematopoietic stem cells (HSC) following conditional deletion of *Pofut1*. However, *Pofut1* deletion by *Mx1-Cre* gives a milder reduction in thymic T cells than deletion of RBP-Jk (25), whereas global deletion of *Pofut1* (26, 27) or RBP-Jk (28) causes similarly severe Notch signaling defects, and embryonic lethality. Thus, loss of O-fucose glycans in HSC does not fully abrogate Notch signaling, suggesting that other O-glycans may support Notch signaling in the absence of POFUT1. POGLUT1 adds O-glucose glycans to Notch receptors. Initially cloned from CD34+ human stem cells (29), POGLUT1 promotes Notch signaling via ligand-dependent and -independent mechanisms (30, 31). Synergism between O-fucose and O-glucose glycans on Notch observed in *Drosophila* (32) and in mammalian cells (33) appears to be due to reduced expression of Notch receptors at the cell surface. By contrast, the absence of O-fucose glycans from Notch receptors in CHO and mouse embryonic stem cells only slightly reduces NOTCH1 cell surface levels (34, 35).

The addition of O-GlcNAc to EGF repeats was first identified in *Drosophila* (36), and the EGF domain specific O-GlcNAc transferase EOGT was subsequently revealed (37, 38). *Eogt* null mice exhibit defective perinatal retinal angiogenesis, similar to that observed in mice with disrupted Notch signaling (39). Cell-based experiments showed that EOGT promotes the binding of DLL Notch ligands and Notch signaling (39). *Eogt* is expressed with *Pofut1* in many cells of the immune system (Figure 1). However, their expression levels vary greatly and inversely in some immune cell types, indicating potentially different functional roles (Figure 1). In this paper, we identify roles for *Eogt* in the regulation of Notch signaling during hematopoiesis, lymphopoiesis and myelopoiesis. In addition, we show that *Eogt* supports Notch signaling in the absence of *Pofut1* and O-fucose glycans.

Methods

Mice

Mice with an inactivating mutation in the *Eogt* gene were generated at Nagoya University and previously described (39). *Pofut1*[F/F] mice were also previously described (26). Transgenic mice expressing *Vav1-iCre* (B6.Cg-*Commd10*$^{Tg(Vav1-icre)A2Kio}$/J Strain) were a kind gift from Britta Will and Paul Frenette at the Albert Einstein College of Medicine, NY, USA. Compound mutant mice termed Pof cKO and EPof dKO, with and without *Vav1-iCre*, were generated by intercrossing. C57Bl/6J male congenic mice expressing CD45.1 (*B6.SJL-Ptprc^a Pepc^b*/BoyJ #002014) were obtained from the Jackson Laboratory (Bar Harbor). Genotyping was performed by PCR of genomic DNA using primers that distinguish wild-type and mutant alleles (Supplementary Table 1). Mice were housed in a barrier facility, allowed to eat and drink ad libitum, and used in experiments at 7–8 weeks of age. All experiments were performed with permission from the Albert Einstein Institutional Animal Care and Use Committee under approved protocol numbers 20170709 and 00001311. Euthanized mice were weighed, bone marrow from femurs, tibias, fibulae, & patullae was isolated, thymus and spleen were weighed before making single-cell suspensions.

Antibodies

Supplementary Table 2 has the full description and commercial source of each antibody used in this work.

Flow cytometry of immune cell subsets

Single-cell suspensions were prepared from bone marrow (BM) by crushing femurs, tibias, fibulae, and patullae in a mortar and rinsing vigorously with 20 ml cold FACS binding buffer (FBB: Hank's balanced salt solution (HBSS) with glucose (Corning), 1 mM CaCl$_2$, 2% bovine serum albumin (BSA, fraction V, Sigma) and 0.05% sodium azide, (pH 7.2–7.4). The BM cell suspension was passed through a 70-μm strainer. Thymus or spleen was weighed and squeezed through a 70 μm strainer in 1 ml FBB. Thymocytes were washed in 10 ml cold FBB twice. Bone marrow and splenocytes were centrifuged and incubated in 1 ml RBC lysis buffer (eBiosciences) for 3-5 min before adding 10 ml cold FBB. After centrifugation and resuspension in 5 ml cold FBB, single cell suspensions were counted in a Coulter counter. Cells were centrifuged at 4°C, resuspended in 2 ml cold PBS with 1 mM CaCl$_2$ and 1 mM MgCl$_2$, pH 7.2, centrifuged and resuspended in 100 μl Zombie NIR dye for live/dead assessment, according to the manufacturer's protocol (Zombie NIR Fixable Viability Kit, BioLegend). After 30 min at 4°C in the dark, 2 ml cold FBB was added. Cells were centrifuged at 4°C, resuspended in 4% paraformaldehyde (PFA, Emsdiasum) in PBS pH 7.2, and incubated 15 min at 4°C in the dark. Cells were washed twice with 2 ml cold FBB, resuspended at 10^6 cells/ml in FBB and stored at 4°C for up to 3 months. For analysis by flow cytometry, ~10^6 cells were washed with 1 ml FBB, resuspended in 90 μl FBB containing 1 μl Fc block (rat-anti-mouse CD16/CD32), and incubated for 15 min on ice. Abs diluted in FBB (10 μl) were added and the reaction mix was incubated for 30 min at 4°C. Cells were washed twice in 1 ml FBB and resuspended in ~500 μl FBB. For all samples, immunofluorescence was analyzed using a Cytek^{TM} Aurora or BD LSRII flow cytometer and data FCS files were analyzed using FlowJo software (Tree Star). Gating strategies shown in Supplementary Figures 1–3 were based on previous work (16, 40, 41) and include the Abs used in the analysis of BM, thymus or spleen immune cell subsets. Data on live cells were collected as frequency percent based on gating strategies. Absolute cell numbers in the different immune cell subsets were calculated from the starting number of live cells and the frequency percent of each subset. Significant differences between genotypes in either frequency percent or absolute cell number are highlighted in the main text while complementary data are presented in supplementary figures as described in the text.

Bone marrow transplantation

Cell suspensions from bone marrow of 7–8 week *Eogt*^{+/-} and *Eogt*^{-/-} males were prepared as described above. Approximately 3x10^6 cells were resuspended in 50 μl sterile HBSS (Gibco) and injected using a 28-gauge insulin needle via the retro-orbital plexus

into CD45.1+ C57BL/6 lethally irradiated recipients. A split dose of 550 rads γ-irradiation per recipient male was given twice, with a 16 h interval. After 7 weeks, recipients were euthanized, bone marrow, thymus, and spleen were analyzed for lymphoid and myeloid cell subsets by flow cytometry after gating on donor-derived cells positive for anti-CD45.2-Pacific Blue.

Isolation of CD4/CD8 double negative T cells

Fresh thymocytes were resuspended in isolation buffer (PBS lacking cations, pH 7.2-7.4, containing 0.1% BSA, 2 mM EDTA and 1 mg/ml glucose) on ice. For T cell depletion, ~3-5x10^7 thymocytes were incubated with 20 μg anti-CD4 (rat IgG2b clone GK1.5, BioXCell) and 37.5 μg anti-CD8a (rat IgG2a clone 53-6.72; BioXCell) in 5 ml buffer for 20 min at 4°C with tilted rotation. After centrifugation, cells were resuspended in 5 ml buffer, and incubated with 250 μl sheep anti-rat IgG Dynabeads (Thermo Fisher Scientific) for 30 min at 4°C with tilted rotation. The tube was placed in a magnet for 2 min, unbound cells were centrifuged and resuspended in 250 μl Dynabeads for a second 30 min incubation at 4°C. After Dynabeads removal, unbound DN T cells were centrifuged, counted and RNA was extracted from the cell pellet with 1 ml TRIZOL (Ambion) as described below.

Quantitative RT-PCR

DN T cells from ~3-5x10^7 thymocytes were pipetted vigorously in 1 ml TRIZOL and incubated for 5 min at RT before adding 200 μl chloroform. Tubes were vortexed for 15 sec, incubated at RT for 2–3 min, and centrifuged at 12,000 × g for 15 min at 4°C. The aqueous phase was transferred to a new tube, and 500 μl isopropanol was added. Samples were incubated for 10 min on ice and centrifuged at 12,000 × g for 10 min at 4°C and the supernatant discarded. The RNA pellet was washed once with 1 ml 70% ethanol. Samples were vortexed for 10 sec and centrifuged at 7,500 × g for 5 min at 4°C and the supernatant discarded. The RNA pellet was air-dried for 5–10 min and dissolved in 50 μl RNase-free water. Samples were placed in a 55-60°C water bath for 15-20 min and the RNA concentration determined by Nanodrop. cDNA was prepared from ~250 ng RNA using the ReverTra Ace® qPCR RT Master Mix with gDNA Remover (Dc. DiagnoCine) following the manufacturer's protocol. Each sample was assayed in triplicate using a 384 well plate. Relative gene expression was calculated in relation to *Hprt* and *Gapdh* by the log2 dCCT method. Primer sequences used for qRT-PCR are in Supplementary Table 1.

Histopathology

Spleen was collected, weighed, washed and stored in 10% natural buffered formalin (NBF) at 4°C. The samples were processed for paraffin embedding and longitudinal tissue sections (5 μm) were stained with hematoxylin and eosin (H&E), scanned by

the 3D Histech P250 High-Capacity Slide Scanner and analyzed using Case Viewer 2.4 software.

Notch ligand binding assay

Soluble Notch ligands DLL1-Fc (#10184-DL-050), JAG1-Fc (#1277-JG-050), and JAG2-Fc (#1726-JG-050) were purchased from R&D Systems, and DLL4-Fc (#DL4-H5259) was purchased from Acro-biosystems. Single-cell suspensions from thymus were washed in FBB at 4°C and fixed in PBS-buffered 4% PFA for 15 min at 4°C, washed twice with FBB and stored in FBB at 4°C. For analysis, ~0.5-1x10^6 fixed thymocytes were washed with FBB, and incubated with 40 μl FBB and 1 μl FcR blocking solution (rat-anti-mouse CD16/CD32) on ice for 15 min. Thereafter, the cells were incubated in 60 μl FBB containing anti-CD4-FITC (1:400), anti-CD8a-PerCp-Cy5.5 (1:400), and 0.75 μg DLL4-Fc, or 1.5 μg of DLL1-Fc, JAG1-Fc, or JAG2-Fc. After incubation at 4°C for ~30 min, cells were washed with 1 ml FBB and incubated with anti-IgG-APC and anti-IgG-DyLight 405 (Fc-specific) Ab (1:100) at 4°C for 30 min. The cells were then washed with 1 ml FBB, resuspended in 500 μl FBB and analyzed in a flow cytometer (Cytek^{TM}, Aurora). For detection of NOTCH1 at the cell surface, fixed thymocytes cells were incubated with FcR-block rat-anti-mouse CD16/CD32 (1:100) followed by anti-CD4-FITC mAb (1:400), anti-CD8a-PerCp-Cy5.5 (1:400), sheep anti-mouse NOTCH1 Ab (1:50) at 4°C for 30 min, washed, and incubated with rhodamine Red-X-conjugated donkey anti-sheep IgG (1:100) at 4°C for 30 min. Cells were washed with 1 ml FBB, resuspended in 500 μl FBB and analyzed in a flow cytometer (Cytek^{TM}, Aurora).

Statistics

Comparisons are presented as mean ± SEM. Significance was determined by both two-tailed and one-tailed (denoted by parentheses) unpaired, parametric, Student t-test analysis (unless otherwise noted) using Prism software version 9.1.

Results

Loss of *Eogt* affects myelopoiesis and lymphopoiesis

Initial comparisons of *Eogt*^{+/+} and *Eogt*^{+/-} heterozygotes revealed no significant differences in T, B and myeloid subset populations in either absolute cell numbers or in the frequency % of different cell subsets (Supplementary Figure 4 and not shown). Therefore, data from *Eogt*^{+/+} and *Eogt*^{+/-} mice were combined as Control. Thymus and spleen weights, as well as bone marrow (BM) cellularity, were similar in *Eogt* null and Control mice (Supplementary Figure 5A). In bone marrow, the absolute numbers of CD19+/B220+ B cells, and CD11b+/Gr1+ granulocytes were significantly increased in the *Eogt*^{-/-} population (Figure 2A). In *Eogt*^{-/-} thymus, the frequency % of CD4/CD8 double negative 1 (DN1) T cell progenitors was reduced, although the absolute number

of DN1 T cells was unchanged (Supplementary Figure 5B). The absolute number of DN2 T cell progenitors was strikingly reduced in *Eogt* null cells, while the absolute number of DN4 T cells was significantly increased (Figure 2B). By contrast, the numbers of early T cell progenitors (ETP) and DN3 T cells were unchanged (Supplementary Figure 5B). The proportion of double positive (DP) T cells was slightly decreased, while CD4+ and CD8+ single positive (SP) T cells were increased in *Eogt*^{-/-} thymocytes (Figure 2B). These effects were also observed in mice lacking the three Fringe genes (*Fng* tKO) (16, 42). Consistent with inhibition of Notch signaling in the *Eogt* null thymus, there was a significant increase in thymic B cells (CD19+/B220+) and the frequency of myeloid cells (CD11b+) (Figure 2B), but no change in natural killer (NK) T cells (Supplementary Figure 5B). In spleen, no histopathological changes were observed in Control versus *Eogt*^{-/-} sections (n=3 for each, not shown), and the absolute numbers of T cells, B cells, marginal zone progenitors (MZ-P) and myeloid cell subsets were similar in Control versus *Eogt*^{-/-} mice (Supplementary Figure 5C). However, significant increases were observed in the absolute number of follicular B (Fo-B), MZ-B, CD19+ and B220+ B cells in *Eogt*^{-/-} mice (Figure 2C). By contrast, a decrease in the frequency % of natural killer T cells (NK1.1+) and dendritic cells (CD11b/c+) was observed (Figure 2C). Thus, EOGT and O-GlcNAc glycans are required for the optimal generation of lymphoid and myeloid cells from HSC.

The *Eogt* null phenotype is largely cell autonomous

To determine whether the *Eogt* null phenotype was cell intrinsic, bone marrow (BM) transplantation was performed from CD45.2+ *Eogt*^{+/-} and *Eogt*^{-/-} donor males into CD45.1+ male hosts. *Eogt*^{-/-} CD45.2+ donor BM cells reconstituted CD45.1+ hosts to ~57% in bone marrow (Figure 3A), ~80% in thymus and ~64% in spleen (not shown). Thus, host-derived *Eogt*^{+/+} cells contributed to each of these populations in recipients. In recipient bone marrow, no changes were seen in B cells (CD19+/B220+) or granulocytes (CD11b+/Gr-1+) from *Eogt*^{-/-} donor BM compared to *Eogt*^{+/-} BM (not shown); in recipient thymus, *Eogt*^{-/-} donor BM generated significantly fewer DN2 and DN3 T cell progenitors compared to *Eogt*^{+/-} donor BM (Figure 3B); and in spleen, *Eogt*^{-/-} donor BM generated CD19+ cells and Gr-1+ granulocytes in significantly increased numbers compared to *Eogt*^{+/-} donor BM (Figure 3C). Thus, the phenotype of *Eogt*^{-/-} BM recipients was somewhat milder, than the *Eogt* null phenotype. This could reflect the presence of *Eogt*^{+/+} host cells, and/or rescuing effects of the wild type host stroma. Nevertheless, key aspects of the *Eogt* null phenotype were transferred by *Eogt*^{-/-} BM.

## Notch signaling is reduced in *Eogt*^{-/-} DN T cell progenitors

Notch ligand binding was examined using thymic DN T cell progenitors from 7-8 week *Eogt*^{+/-} and *Eogt*^{-/-} mice. No significant changes were observed in either NOTCH1 cell surface expression, or the binding of soluble ligands DLL1, DLL4, JAG1 or JAG2 between Eogt^{+/-} and *Eogt*^{-/-} DN T cell progenitors (Figure 4A). However, there were significant reductions in the expression of two Notch target genes, *Hes1* and *Il2ra*, consistent with reduced Notch signaling (Figure 4B). The expression of *Il2ra* was also reduced in DN T cell progenitors from mice lacking the three Fringe genes, along with *Dtx1*, although not *Hes1* (16). The reduction in Notch signaling target gene expression in *Eogt* null T cell progenitors, the changes in T cell subset numbers and frequencies, and the increased numbers of B and myeloid cells observed in *Eogt*^{-/-} thymus, indicate that EOGT and O-GlcNAc glycans are necessary for optimal Notch signaling and T cell development. The altered B cell and myeloid subsets in spleen of *Eogt*^{-/-} mice are also consistent with reduced Notch signaling. Finally, the B cell and myeloid hyperplasia in *Eogt*^{-/-} BM indicate that Notch signaling is required for regulating the differentiation of certain progenitors during hematopoiesis.

Eogt supports lymphoid and myeloid development in HSC lacking *Pofut1*

Previous work showed that inactivation of *Pofut1* using *Mx1-Cre* causes a reduction in T lymphopoiesis in thymus and myeloid hyperplasia in bone marrow (24). In another study, conditional deletion of *Pofut1* in bone marrow was shown to cause a milder T cell phenotype than deletion of RBP-Jk (25). To determine whether *Eogt* and O-GlcNAc glycans support Notch signaling and hematopoiesis in the absence of *Pofut1*, we used *Vav1-iCre* transgenic mice to generate conditional deletion (cKO) of *Pofut1* (henceforth referred to as Pof cKO), and deletion of both *Eogt* and *Pofut1* (henceforth referred to as EPof dKO), in hematopoietic stem cells. The absolute number of BM cells was significantly increased in both Pof cKO and EPof dKO mice (Figure 5). Gating strategies used to define HSC, HSPC, myeloid and lymphoid cell subsets in BM are shown in Supplementary Figure 6. Short-term (ST)-HSC, and LSK (Lineage-Sca1+cKit+) cell numbers were increased in both Pof cKO and EPof dKO mutants, but the frequency % of HSPCs was increased only in EPof dKO BM (Figure 5). By contrast, the frequency % of MPP subsets was reduced except for a small increase in the MPP3 population in EPof dKO BM (Figure 5). The frequency % of lymphoid primed multipotent progenitor cells (MPP4/LMPP) and common myeloid precursors (CMP) were reduced in Pof cKO and further reduced in EPof dKO BM, and megakaryocyte erythrocyte progenitors (MEP) were decreased in both single and double mutants (Figure 5). By contrast, the frequency % of granulocyte-monocyte progenitors (GMP) was increased in Pof cKO (as observed previously (24)), and further increased in EPof dKO BM (Figure 5 and Supplementary Figure 7). The proportion of CD11b+/Gr-1+ granulocytes was increased, but the proportion of common lymphoid progenitors (CLP) was reduced in EPof dKO BM (Figure 5). The frequency % of T- and B-cells in BM was also decreased in EPof dKO mice (Figure 5). NOTCH1 was expressed at the surface of Lin-Sca1+ cells which were increased in frequency in Pof cKO and EPof dKO BM
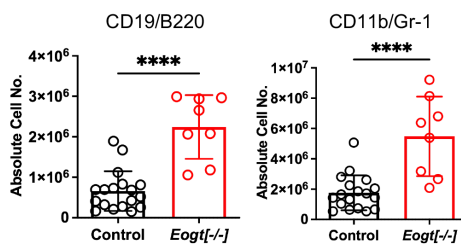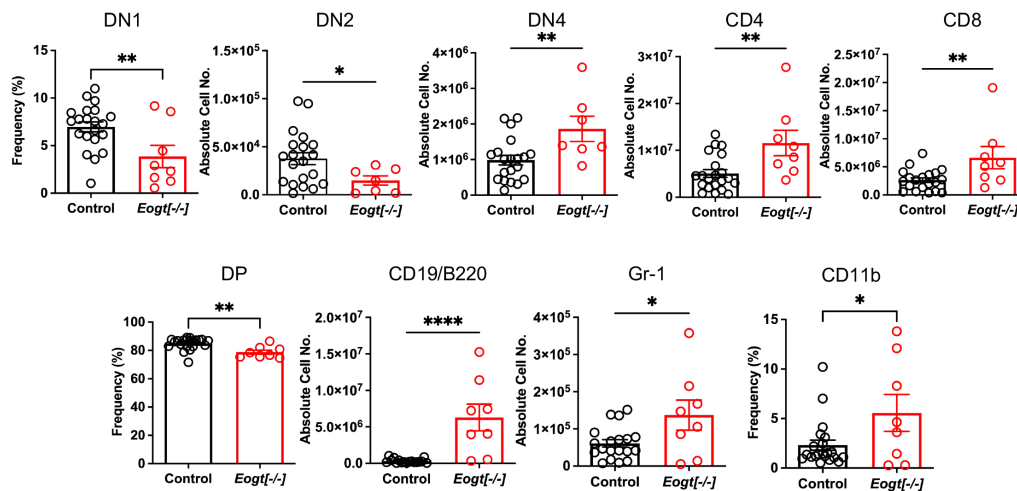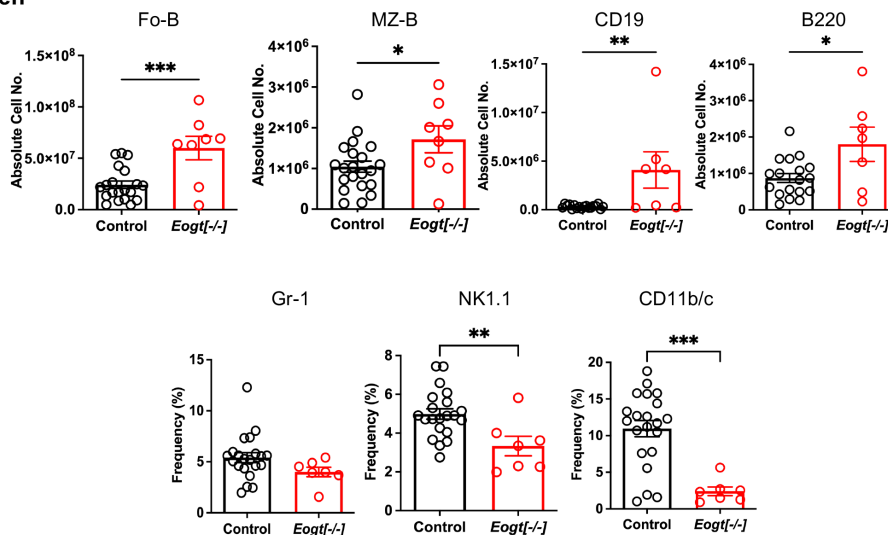
FIGURE 2

Altered lymphoid and myeloid subsets in mice lacking *Eogt* and O-GlcNAc glycans. **(A)** Absolute cell numbers or frequency % for lymphoid and myeloid cell subsets in bone marrow that differed between Control (*Eogt*^{+/+} and *Eogt*^{+/-}) and *Eogt*^{-/-} mice. See Supplementary Figure 1 for gating, Supplementary Figure 4 for *Eogt*^{+/+} versus *Eogt*^{+/-} data and Supplementary Figure 5 for BM cellularity. **(B)** Absolute cell numbers or frequency % for lymphoid and myeloid cell subsets in thymus that differed between Control and *Eogt*^{-/-} mice. See Supplementary Figure 2 for gating, Supplementary Figure 4 for *Eogt*^{+/+} versus *Eogt*^{+/-} data and Supplementary Figure 5 for subsets that did not differ significantly. **(C)** Absolute cell numbers or frequency % for lymphoid and myeloid cell subsets in spleen that differed between Control and *Eogt*^{-/-} mice. See Supplementary Figure 3 for gating, Supplementary Figure 4 for *Eogt*^{+/+} versus *Eogt*^{+/-} data and Supplementary Figure 5 for subsets that did not differ significantly. Each symbol represents a mouse of 7-8 weeks. Data are presented as mean ± SEM. *p <0.05, **p<0.01,***p<0.001, ****p<0.0001 based on two-tailed Student's t test.
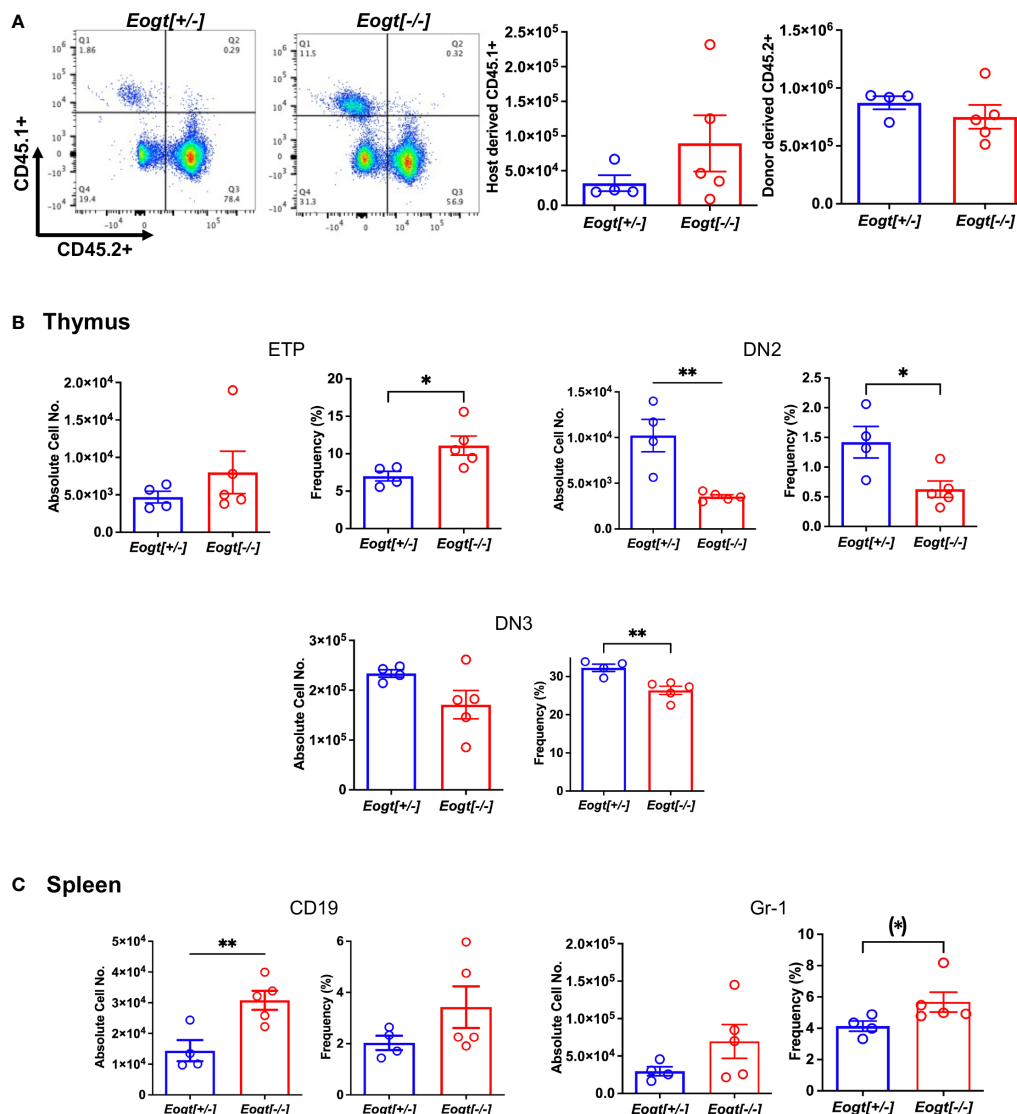
FIGURE 3

The *Eogt* null phenotype is largely cell autonomous. Bone marrow cells (3X10⁶) from *Eogt*^{+/-} or *Eogt*^{-/-} mice expressing CD45.2 were injected via the retro-orbital plexus into lethally-irradiated, wild-type recipient males expressing CD45.1. Recipient BM, thymus and spleen were analyzed 7 weeks after transplantation. **(A)** Flow cytometry profile and histograms of bone marrow from recipient mice (CD45.1+) that received BM from *Eogt* [+/-] or *Eogt*^{-/-} mice. The approximate donor contribution was 78% for *Eogt*^{+/-} and 57% for *Eogt*^{-/-} of recipient BM. **(B)** Absolute cell number and frequency % of T cell progenitors in thymus that differed when derived from *Eogt*^{+/-} versus *Eogt*^{-/-} donor bone marrow. **(C)** Absolute cell number and frequency % of B cells and granulocyte subsets in spleen that differed when derived from *Eogt*^{+/-} versus *Eogt*^{-/-} donor bone marrow. Each symbol represents a mouse of 7-8 weeks. Data are presented as mean $\pm$ SEM. *p <0.05, **p<0.01 based on two-tailed Student's t test. (*) p <0.05 based on one-tailed Student's t test.

(Supplementary Figure 8). Binding of DLL1 and DLL4 Notch ligands was low and similar in control and mutant Sca1+ cells (Supplementary Figure 8).

Highly disrupted development of T cells in EPof dKO thymus

Deletion of *Pofut1* in HSC via *Vav1-iCre* led to a marked decrease in thymus weight and a similar reduction was observed in EPof dKO thymus (Figure 6A). The reduced size was accompanied by a dramatic change in T cell maturation (Figure 6B). Early thymic progenitors (ETP) were greatly decreased in absolute number, and each DN T cell progenitor population (DN1 to DN4) was also reduced in absolute cell number in Pof cKO, and even further reduced in EPof dKO thymocytes (Figure 6C and Supplementary Figure 9). Interestingly, however, the frequency % of DN4 T cells in both single and double mutant thymocytes was increased relative to control (Supplementary Figure 9), as observed in thymus lacking all Fringe activities (16). The DN T cell population, which includes few DN T cell progenitors and all the non-T cell populations, was greatly
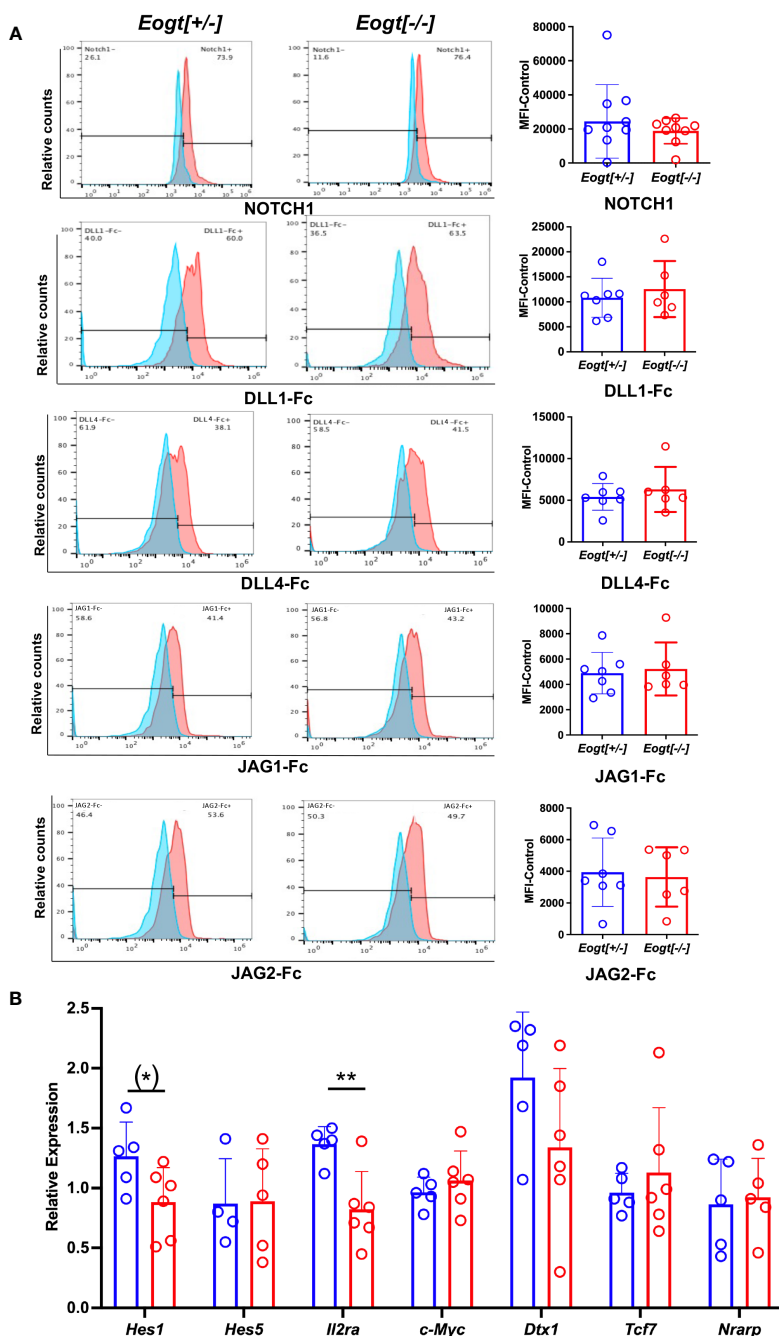
FIGURE 4

Notch signalling in *Eogt* null T cell progenitors. Representative flow cytometry profiles and histogram quantification of **(A)** Cell surface NOTCH1, or binding of DLL1-Fc, DLL4-Fc, JAG1-Fc and JAG2-FC to fixed CD4/CD8 DN T cell progenitors from *Eogt*^{+/-} or *Eogt*^{-/-} mice. Mean fluorescence index (MFI) for anti-Fc Ab was subtracted from MFI for Notch ligand or NOTCH1 Ab (MFI-control). Symbols represent *Eogt*^{+/-} (blue circles) and *Eogt*^{-/-} (red circles) DN T cells. Fixed cells had been stored for up to 3 months at 4°C. **(B)** Transcripts from DN T cell progenitors of *Eogt*^{+/-} or *Eogt*^{-/-} mice were subjected to qRT-PCR as described in Materials and Methods. Relative expression was determined based on the average delta Ct obtained for *Gapdh* and *Hprt* combined. Each symbol represents a mouse of 7-8 weeks. Data are presented as mean $\pm$ SEM. *p <0.05, **p<0.01 based on two-tailed Student's t test or (*) p <0.05 based on one-tailed Student's t test.

increased in Pof cKO and EPof dKO, as expected. This reflected loss of Notch signaling leading to the generation of B cell, myeloid and NK cell subsets in thymus (Figure 6D and Supplementary Figure 9). Notably, effects were more severe in EPof dKO than Pof cKO thymus, suggesting that the loss of Notch signaling was greater in EPof dKO thymus.

Defective B, T and myeloid cell development in EPof dKO spleen

Both Pof cKO and EPof dKO mice had an enlarged spleen (Figure 7A). Absolute numbers of splenocytes and spleen weight were increased in Pof cKO, and further increased in EPof dKO mice
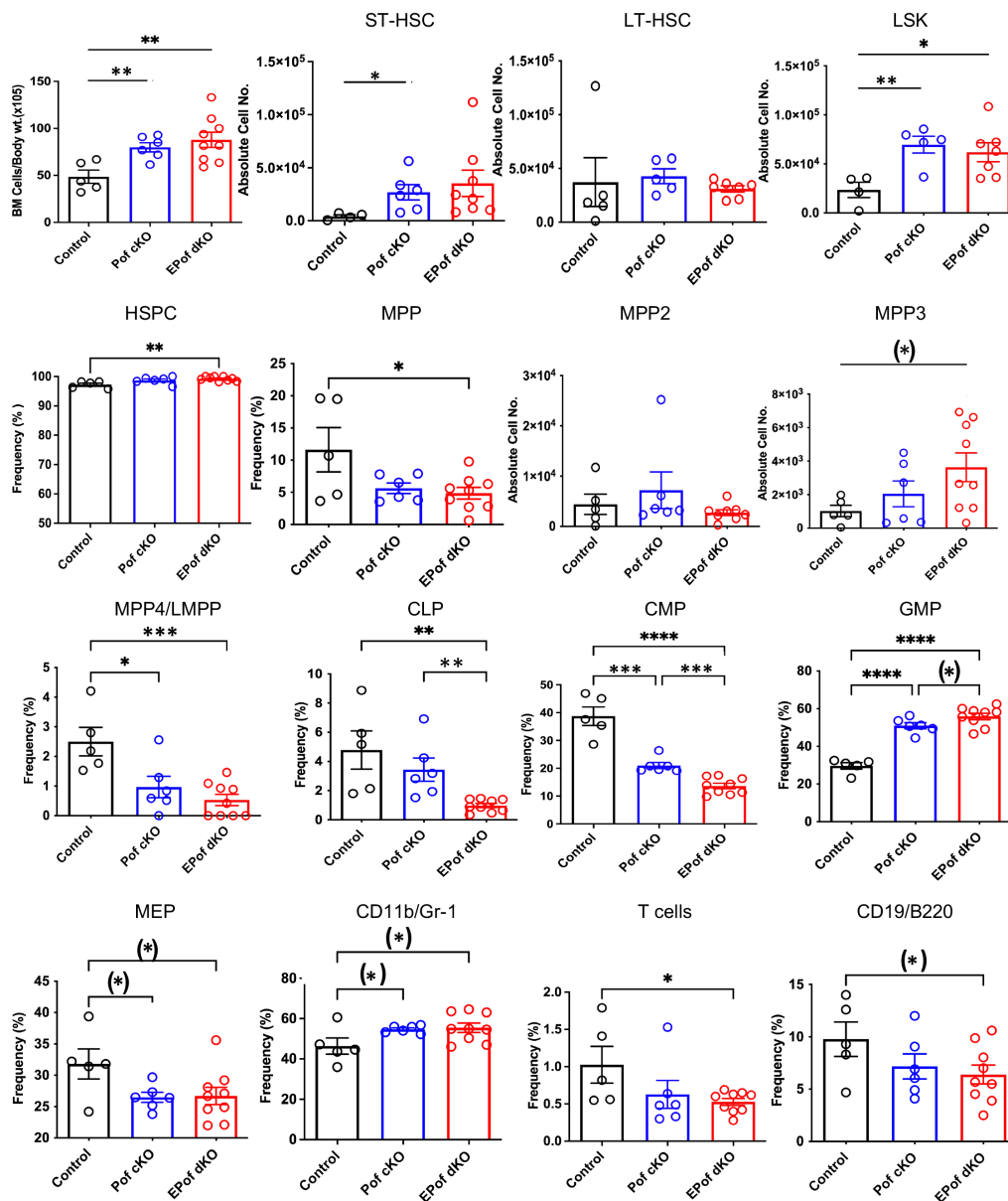
FIGURE 5

Hematopoiesis in EPof dKO bone marrow. Hematopoiesis was analyzed in bone marrow of *Eogt*^{+/-}*Pofut1*[F/F] (Control), *Pofut1*[F/F] : *Vav1-iCre* (Pof cKO) and *Eogt*^{-/-}*Pofut1*[F/F] : *Vav1-iCre* (EPof dKO) mice. Absolute numbers or frequency % of hemopoietic cell subsets in bone marrow are shown. Gating strategies are shown in Supplementary Figure 6 and additional data are shown in Supplementary Figure 7. Short term-hemopoietic stem cells (ST-HSC), long-term hemopoietic stem cells (LT-HSC), Lin-Sca1+c-Kit+ (LSK) cells, hematopoietic stem progenitor cells (HSPCs), multipotent progenitor-2, -3, -4 (MPP2, -3, -4), lymphoid primed multipotent progenitor cell (LMPP), common lymphoid progenitor (CLP), common myeloid progenitor (CMP), granulocyte monocyte progenitor (GMP), megakaryocyte erythrocyte progenitor (MEP), T cells, B cells and myeloid cells. Each symbol represents a mouse of 7-8 weeks. Data are presented as mean ± SEM. *p <0.05, **p<0.01, ***p<0.001, ****p<0.001 based on two-tailed Student's t test or (*) p <0.05 based on one-tailed Student's t test.

(Figure 7B). Histological analysis revealed extramedullary hematopoiesis in both Pof cKO and EPof dKO spleens, with larger areas of extramedullary hematopoiesis observed in EPof dKO spleen (Figure 7A).

The absolute numbers of single positive CD4+ and CD8+ T cells were significantly reduced in Pof cKO, and further reduced in EPof dKO spleen (Figure 7C and Supplementary Figure 10). While CD19+ and B220+ B cells were proportionally increased in

both Pof cKO and EPof dKO spleen, the frequency % of the CD19+/B220+ B cell population was reduced (Figure 7D). The frequency of Fo-B and the number of MZ-B cells were also reduced (Figure 7D and Supplementary Figure 10). While the absolute number of MZ-P cells did not change in the mutants, the frequency % of MZ-P precursors was increased in EPof dKO spleen (Figure 7 and Supplementary Figure 10). Myeloid cell subsets such as dendritic cells (CD11b/c+) and Gr-1+
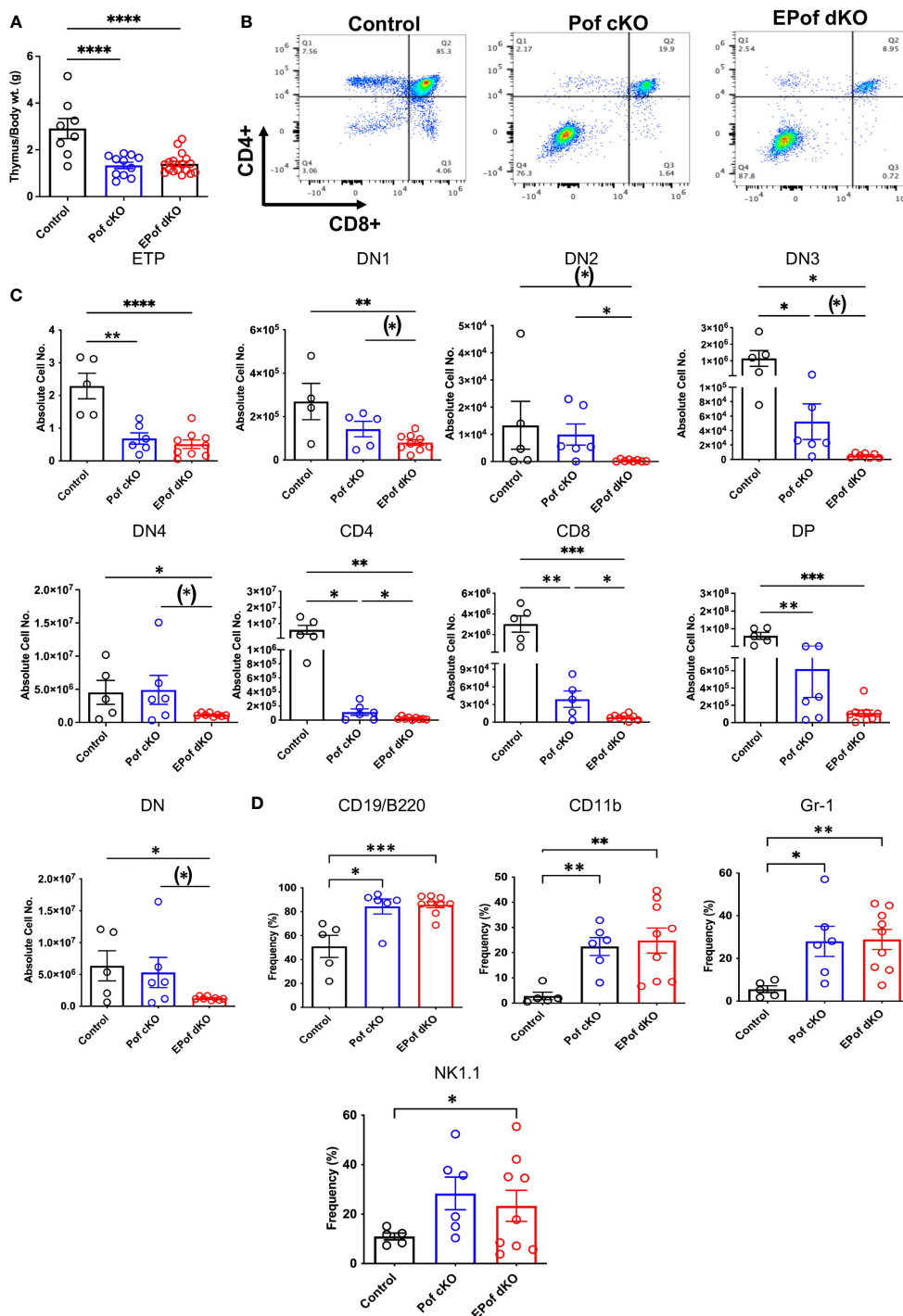
FIGURE 6

Impaired T cell development in Pof cKO thymus is worse in EPof dKO thymus. **(A)** Thymus weight compared to body weight. **(B)** Representative flow cytometry profiles of thymocytes using Abs to CD4 and CD8 cell surface markers after gating on live cells. **(C)** Absolute cell numbers or frequency % of T cell subsets that differed between Control and either mutant. ETP (DN1 cells that were cKit/CD117+), DN1 (CD44+CD25-), DN2 (CD44+CD25+), DN3 (CD44-CD25+), and DN4 (CD44-CD25-) T cell progenitors, DN (CD4 and CD8 double negative), DP (CD4 and CD8 double positive). **(D)** Absolute cell numbers or frequency % of B cell and myeloid cell subsets that differed from control are shown. Additional data are shown in Supplementary Figure 9. Each symbol represents a mouse of 7-8 weeks. Data are presented as mean ± SEM. *p <0.05, **p<0.01, ***p<0.001, ****p<0.001 based on two-tailed Student 'st test or (*) p <0.05 based on one-tailed Student's t test.

FIGURE 7
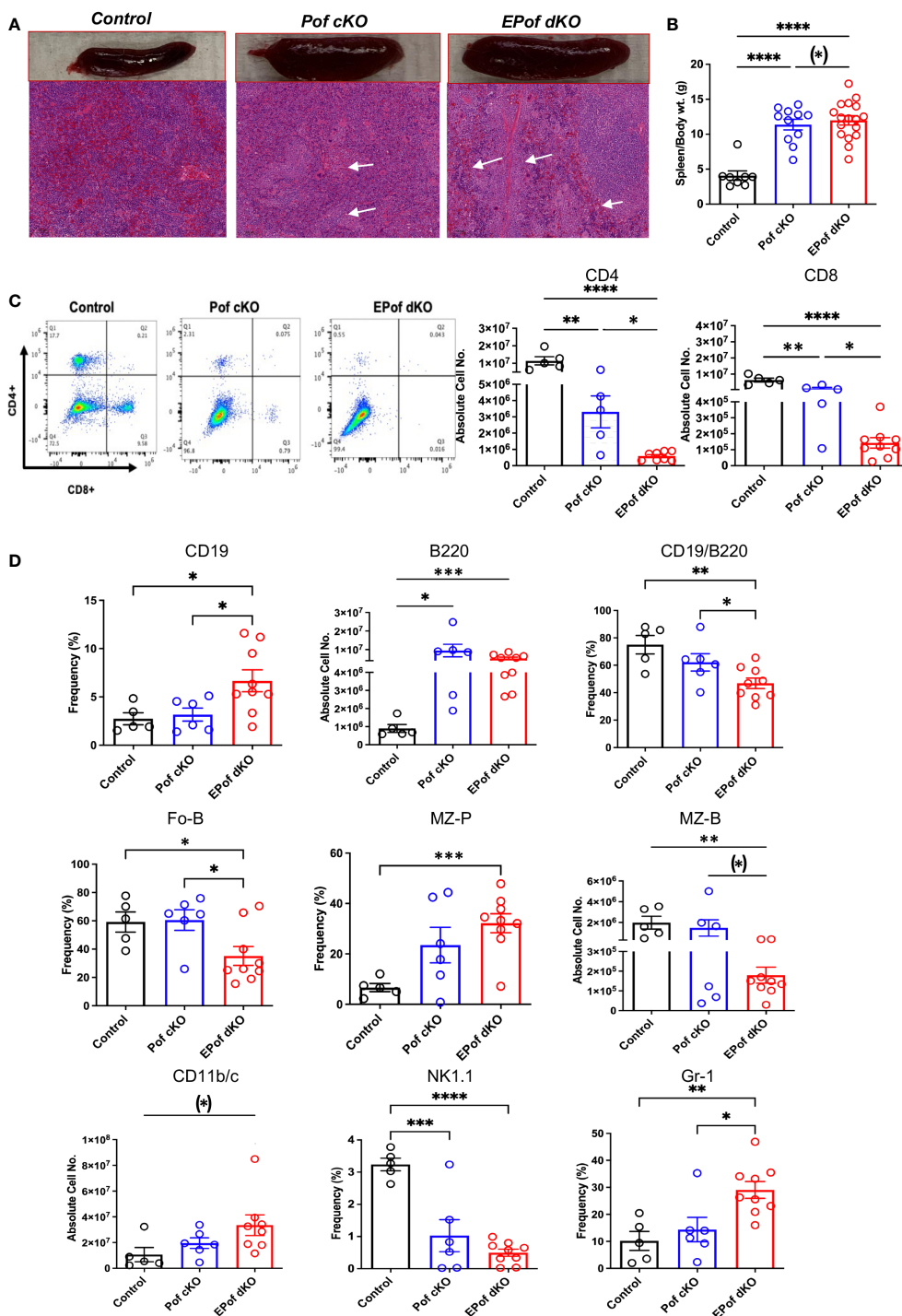
Impaired B and T cell development in Pof cKO spleen is worse in EPof dKO spleen. **(A)** Images of spleen sections stained by H&E revealing splenomegaly and extramedullary hematopoiesis (Bars represent 100 μm). **(B)** Spleen weight compared to body weight. **(C)** Flow cytometric profiles and histogram quantification for CD4 versus CD8 cell surface expression after gating on live cells. **(D)** Absolute cell numbers or frequency % of splenic lymphoid and myeloid cell subsets that differed from control are shown. CD19/B220 (B cells), Fo-B (follicular B cells), MZ-B (marginal zone-B cells), MZ-P (marginal zone precursors), CD11b/c (dendritic cells), NK1.1 (natural killer T cells) and Gr-1 (granulocytes). Additional data are shown in Supplementary Figure 10. Each symbol represents a mouse of 7-8 weeks. Data are presented as mean $\pm$ SEM. *p <0.05, **p<0.01, ***p<0.001, ****p<0.001 based on two-tailed Student's t test or (*) p <0.05, based on one-tailed Student's t test.

granulocytes were increased in greater proportion in EPof dKO compared to Pof cKO spleens. Natural killer T cells were reduced in frequency in both Pof cKO and EPof dKO spleens (Figure 7D and Supplementary Figure 10).

Discussion

Defining specific roles for the glycans that regulate Notch signaling in lymphoid and myeloid development facilitates our understanding of cell fate decisions controlled by Notch signaling, and of potential consequences for people with congenital diseases that perturb Notch signaling (2, 43). Several congenital diseases inhibit the synthesis or extension of O-glycans that regulate Notch signaling and may induce immune cell defects. Mutations in *EOGT* cause Adams Oliver syndrome (44) and autosomal dominant mutations in *POFUT1* cause Dowling Degos Disease 2 (DDD2) (45). Here we show that the generation of certain lymphoid and myeloid subsets in bone marrow, thymus and spleen was perturbed in mice lacking *Eogt*. In bone marrow, loss of EOGT caused increased numbers of B cells and granulocytes. In thymus, the phenotype of *Eogt* null mice was similar, but not identical to, mice which lack all three Fringe genes (*Fng* tKO) (16). T cell progenitors DN1 and DN2 were reduced in frequency or absolute number, whereas DN4 T cell progenitors were increased, DP T cells were slightly reduced in frequency, and CD4+ and CD8+ SP T cells were increased in absolute numbers. Inhibition of Notch signaling in thymus is well known to lead to the generation of B cells and myeloid cells in thymus (9, 11, 46, 47). *Eogt* null thymus contained significantly increased numbers of B cells and granulocytes, and an increased frequency of myeloid cells. In spleen, *Eogt* null splenocytes included increased numbers of several B cell subsets, although there were no effects on T cells, unlike in *Fng* tKO mice which had a reduced frequency of T cells in spleen (16). Deletion of RBP-Jk by *Vav1-iCre* results in an increased frequency of CD19+ B cells (48), also observed in *Eogt* null spleen. *Eogt* null mice showed increased absolute numbers of CD19+ B cells, increased Fo-B cells, and a decrease in natural killer T-cells and dendritic cells in the spleen. The overall *Eogt* null phenotype was largely cell autonomous following bone marrow transplantation. In addition, expression of Notch target genes *Hes1* and *Il2ra* was reduced, similar to *Fng* tKO DN T cell progenitors that had reduced *Il2ra* and *Dtx1* expression (16). The combined data provide strong evidence that EOGT and O-GlcNAc glycans are required for optimal Notch signaling in the development of lymphoid and myeloid cells from HSC.

Further evidence that EOGT and O-GlcNAc glycans support Notch signaling in lymphoid and myeloid development was obtained in compound mutant mice lacking *Eogt* and conditionally lacking *Pofut1* in HSC. EPof dKO lymphoid and myeloid populations in BM, thymus and spleen were more affected compared to Pof cKO. We conclude that the loss of *Eogt* and O-GlcNAc glycans in EPof cKO HSC exacerbated the deficits in T, B and myeloid differentiation evident in Pof cKO mice. This result, and our findings that *Eogt* is required for optimal Notch signaling and the differentiation of HSC, provide an explanation for the observation that *Pofut1:Mx1-Cre* T cell deficiencies were not as

severe as those obtained in *RBP-Jk : Mx1-Cre* thymus (25). In the absence of POFUT1 and O-fucose glycans, the O-GlcNAc glycans transferred by EOGT to Notch receptors can support a low but significant level of Notch signaling. Thus, as shown here and discussed in a recent review (49), the O-fucose and O-GlcNAc glycans on Notch act synergistically to provide optimal Notch signaling in lymphopoiesis and myelopoiesis.

The conclusions obtained from these experiments are necessarily limited by the difficulty of demonstrating structural changes in the O-glycans on Notch receptors predicted to change in the absence of relevant glycosyltransferase(s). For example, to obtain sufficient NOTCH1 from splenic T cells for analysis by mass spectrometry, it was necessary to activate the T cells in culture thereby increasing cell surface NOTCH1 by ~ 10-fold (50). Furthermore, the effects of conditional deletion of *Eogt* in HSC would allow us to define the contribution, if any, of *Eogt* null stroma to the *Eogt* null phenotype. It would also be important to determine Notch ligand binding and Notch target gene expression in cells from different HSPC lineages in Pof cKO and EPof dKO mice. Single cell RNA-seq of different mutant HSC and HSPCs would greatly expand our understanding of the pathways affected by altered Notch signaling due to loss of regulation by O-glycans in HSC. Moreover, it would be important to investigate roles for the O-glycans on Notch ligands by deleting *Pofut1*, *Eogt* and related glycosyltransferase genes in stromal cells. Another important question for future work is whether changes in immune subset cell numbers reflect apoptosis or proliferation of one or more populations. This question and changes in Notch target gene expression are difficult to determine because changes in Notch signaling lead to changes in cell fates. For example, thymus lacking POFUT1 or EOGT + POFUT1 has few, if any, T cell progenitors and largely comprises B cells, myeloid and NK cells making comparisons with wild type or *Eogt* null thymocytes meaningless in terms of underlying mechanisms. Thus, the major benefit of the experiments reported here is to pinpoint cell fate decisions regulated differently by the strength of Notch signaling which in turn is regulated by the O-glycans of Notch receptors. In addition, our findings contribute to the growing body of evidence that glycans are integral to the functions of all glycoproteins, glycolipids, glycophosphatidylinositol (GPI)-anchored proteins and proteoglycans. Glycans must be included as essential contributors to life, along with proteins, nucleic acids and lipids, to facilitate progress in the personalized medicines of the future (51).

Data availability statement

The raw data supporting the conclusions of this article will be made available by the authors, without undue reservation.

Ethics statement

The animal studies were approved by Institutional Animal Care and Use Committee. The studies were conducted in accordance with the local legislation and institutional requirements. Written informed consent was not obtained from the owners for the

participation of their animals in this study because the mice were bred in my colony at Albert Einstein following approval of the IACUC. I am therefore the owner.

Author contributions

Conceptualization, PS; Methodology, PS and AT; Investigation, AT and PS; Visualization AT and PS; Funding acquisition, PS; Project administration, PS; Supervision, PS; Writing – original draft, AT; review and editing, PS and AT. All authors contributed to the article and approved the submitted version.

Funding

Acknowledgments

Conflict of interest

The authors declare that the research was conducted in the absence of any commercial or financial relationships that could be construed as a potential conflict of interest.

Publisher's note

All claims expressed in this article are solely those of the authors and do not necessarily represent those of their affiliated organizations, or those of the publisher, the editors and the reviewers. Any product that may be evaluated in this article, or claim that may be made by its manufacturer, is not guaranteed or endorsed by the publisher.

Supplementary material

The Supplementary Material for this article can be found online at: https://www.frontiersin.org/articles/10.3389/fimmu.2023.1097332/full#supplementary-material

References

1. Kopan R. Notch signaling. In: *Cold spring harbor perspectives in biology*, vol. 4. (2012). p. a011213–a. doi: 10.1101/cshperspect.a011213

2. Varshney S, Stanley P. Multiple roles for O-glycans in Notch signaling. *FEBS Lett* (2018) 592(23):3819–34. doi: 10.1002/1873-3468.13251

3. Pandey A, Niknejad N, Jafar-Nejad H. Multifaceted regulation of Notch signaling by glycosylation. *Glycobiology* (2021) 31(1):8–28. doi: 10.1093/glycob/cwaa049

4. Luca VC, Jude KM, Pierce NW, Nachury MV, Fischer S, Garcia KC. Structural biology. Structural basis for Notch1 engagement of Delta-like 4. *Science* (2015) 347 (6224):847–53. doi: 10.1126/science.1261093

5. Luca VC, Kim BC, Ge C, Kakuda S, Wu D, Roein-Peikar M, et al. Notch-Jagged complex structure implicates a catch bond in tuning ligand sensitivity. *Science* (2017) 355(6331):1320–4. doi: 10.1126/science.aaf9739

6. Kovall RA, Gebelein B, Sprinzak D, Kopan R. The canonical Notch signaling pathway: structural and biochemical insights into shape, sugar, and force. *Dev Cell* (2017) 41(3):228–41. doi: 10.1016/j.devcel.2017.04.001

7. Ho DM, Guruharsha KG, Artavanis-Tsakonas S. The Notch interactome: complexity in signaling circuitry. *Adv Exp Med Biol* (2018) 1066:125–40. doi: 10.1007/978-3-319-89512-3_7

8. Lampreia FP, Carmelo JG, Anjos-Afonso F. Notch signaling in the regulation of hematopoietic stem cell. *Curr Stem Cell Rep* (2017) 3(3):202–9. doi: 10.1007/s40778-017-0090-8

9. Vanderbeck A, Maillard I. Notch signaling at the crossroads of innate and adaptive immunity. *J Leukoc Biol* (2021) 109(3):535–48. doi: 10.1002/JLB.1RI0520-138R

10. Koch U, Fiorini E, Benedito R, Besseyrias V, Schuster-Gossler K, Pierres M, et al. Delta-like 4 is the essential, nonredundant ligand for Notch1 during thymic T cell lineage commitment. *J Exp Med* (2008) 205(11):2515–23. doi: 10.1084/jem.20080829

11. Feyerabend TB, Terszowski G, Tietz A, Blum C, Luche H, Gossler A, et al. Deletion of Notch1 converts pro-T cells to dendritic cells and promotes thymic B cells by cell-extrinsic and cell-intrinsic mechanisms. *Immunity* (2009) 30(1):67–79. doi: 10.1016/j.immuni.2008.10.016

12. Romero-Wolf M, Shin B, Zhou W, Koizumi M, Rothenberg EV, Hosokawa H. Notch2 complements Notch1 to mediate inductive signaling that initiates early T cell development. *J Cell Biol* (2020) 219(10):e202005093. doi: 10.1083/jcb.202005093

13. Saito T, Chiba S, Ichikawa M, Kunisato A, Asai T, Shimizu K, et al. Notch2 is preferentially expressed in mature B cells and indispensable for marginal zone B lineage development. *Immunity* (2003) 18(5):675–85. doi: 10.1016/s1074-7613(03)00111-0

14. Hozumi K, Negishi N, Suzuki D, Abe N, Sotomaru Y, Tamaoki N, et al. Delta-like 1 is necessary for the generation of marginal zone B cells but not T cells in vivo. *Nat Immunol* (2004) 5(6):638–44. doi: 10.1038/ni1075

15. Tan JB, Xu K, Cretegny K, Visan I, Yuan JS, Egan SE, et al. Lunatic and manic fringe cooperatively enhance marginal zone B cell precursor competition for Delta-like 1 in splenic endothelial niches. *Immunity* (2009) 30(2):254–63. doi: 10.1016/j.immuni.2008.12.016

16. Song Y, Kumar V, Wei H-X, Qiu J, Stanley P. Lunatic, manic, and radical fringe each promote T and B cell development. *J Immunol* (2016) 196(1):232–43. doi: 10.4049/jimmunol.1402421

17. Harvey BM, Haltiwanger RS. Regulation of Notch function by O-glycosylation. *Adv Exp Med Biol* (2018) 1066:59–78. doi: 10.1007/978-3-319-89512-3_4

18. Heng TS, Painter MW. Immunological genome project C. The immunological genome project: networks of gene expression in immune cells. *Nat Immunol* (2008) 9 (10):1091–4. doi: 10.1038/ni1008-1091

19. Rampal R, Luther KB, Haltiwanger RS. Notch signaling in normal and disease states: possible therapies related to glycosylation. *Curr Mol Med* (2007) 7(4):427–45. doi: 10.2174/156652407780831593

20. Ogawa M, Okajima T. Structure and function of extracellular O-GlcNAc. *Curr Opin Struct Biol* (2019) 56:72–7. doi: 10.1016/j.sbi.2018.12.002

21. Yuan JS, Tan JB, Visan I, Matei IR, Urbanellis P, Xu K, et al. Lunatic fringe prolongs Delta/Notch-induced self-renewal of committed alphabeta T-cell progenitors. *Blood* (2011) 117(4):1184–95. doi: 10.1182/blood-2010-07-296616

22. Visan I, Yuan JS, Liu Y, Stanley P, Guidos CJ. Lunatic fringe enhances competition for delta-like notch ligands but does not overcome defective pre-tcr signaling during thymocyte beta-selection in vivo. *J Immunol* (2010) 185(8):4609–17. doi: 10.4049/jimmunol.1002008

23. Visan I, Tan JB, Yuan JS, Harper JA, Koch U, Guidos CJ. Regulation of T lymphopoiesis by Notch1 and Lunatic fringe-mediated competition for intrathymic niches. *Nat Immunol* (2006) 7(6):634–43. doi: 10.1038/ni1345

24. Yao D, Huang Y, Huang X, Wang W, Yan Q, Wei L, et al. Protein O-fucosyltransferase 1 (Pofut1) regulates lymphoid and myeloid homeostasis through modulation of Notch receptor ligand interactions. *Blood* (2011) 117(21):5652–62. doi: 10.1182/blood-2010-12-326074

25. Yu VWC, Saez B, Cook C, Lotinun S, Pardo-Saganta A, Wang Y-H, et al. Specific bone cells produce DLL4 to generate thymus-seeding progenitors from bone marrow. *J Exp Med* (2015) 212(5):759–74. doi: 10.1084/jem.20141843

26. Shi S, Stanley P. Protein O-fucosyltransferase 1 is an essential component of Notch signaling pathways. *Proc Natl Acad Sci* (2003) 100(9):5234–9. doi: 10.1073/pnas.0831126100

27. Okamura Y, Saga Y. Pofut1 is required for the proper localization of the Notch receptor during mouse development. *Mech Dev* (2008) 125(8):663–73. doi: 10.1016/j.mod.2008.04.007

28. Oka C, Nakano T, Wakeham A, de la Pompa JL, Mori C, Sakai T, et al. Disruption of the mouse RBP-J kappa gene results in early embryonic death. *Development* (1995) 121(10):3291–301. doi: 10.1242/dev.121.10.3291

29. Teng Y, Liu Q, Ma J, Liu F, Han Z, Wang Y, et al. Cloning, expression and characterization of a novel human cap10-like gene hclp46 from cd34(+) stem/progenitor cells. *Gene* (2006) 371(1):7–15. doi: 10.1016/j.gene.2005.08.027

30. Acar M, Jafar-Nejad H, Takeuchi H, Rajan A, Ibrani D, Rana NA, et al. Rumi is a cap10 domain glycosyltransferase that modifies Notch and is required for Notch signaling. *Cell* (2008) 132(2):247–58. doi: 10.1016/j.cell.2007.12.016

31. Fernandez-Valdivia R, Takeuchi H, Samarghandi A, Lopez M, Leonardi J, Haltiwanger RS, et al. Regulation of mammalian Notch signaling and embryonic development by the protein O-glucosyltransferase Rumi. *Development* (2011) 138(10):1925–34. doi: 10.1242/dev.060020

32. Matsumoto K, Ayukawa T, Ishio A, Sasamura T, Yamakawa T, Matsuno K. Dual roles of O-glucose glycans redundant with monosaccharide O-fucose on Notch in Notch signaling. *J Biol Chem* (2016) 291(26):13743–52. doi: 10.1074/jbc.M115.710483

33. Takeuchi H, Yu H, Hao H, Takeuchi M, Ito A, Li H, et al. O-glycosylation modulates the stability of epidermal growth factor-like repeats and thereby regulates Notch trafficking. *J Biol Chem* (2017) 292(38):15964–73. doi: 10.1074/jbc.M117.800102

34. Wang Y, Wu B, Lu P, Zhang D, Wu B, Varshney S, et al. Uncontrolled angiogenic precursor expansion causes coronary artery anomalies in mice lacking Pofut1. *Nat Commun* (2017) 8(1):578. doi: 10.1038/s41467-017-00654-w

35. Stahl M, Uemura K, Ge C, Shi S, Tashima Y, Stanley P. Roles of Pofut1 and O-fucose in mammalian Notch signaling. *J Biol Chem* (2008) 283(20):13638–51. doi: 10.1074/jbc.m802027200

36. Matsuura A, Ito M, Sakaidani Y, Kondo T, Murakami K, Furukawa K, et al. O-linked N-acetylglucosamine is present on the extracellular domain of Notch receptors. *J Biol Chem* (2008) 283(51):35486–95. doi: 10.1074/jbc.M806202200

37. Sakaidani Y, Nomura T, Matsuura A, Ito M, Suzuki E, Murakami K, et al. O-linked-N-acetylglucosamine on extracellular protein domains mediates epithelial cell-matrix interactions. *Nat Commun* (2011) 2:583. doi: 10.1038/ncomms1591

38. Müller R, Jenny A, Stanley P. The egf repeat-specific O-GlcNAc transferase and Eogt interacts with Notch signaling and pyrimidine metabolism pathways in drosophila. *PloS One* (2013) 8(5):e62835. doi: 10.1371/journal.pone.0062835

39. Sawaguchi S, Varshney S, Ogawa M, Sakaidani Y, Yagi H, Takeshita K, et al. O-GlcNAc on NOTCH1 EGF repeats regulates ligand-induced Notch signaling and vascular development in mammals. *eLife* (2017) 6. doi: 10.7554/elife.24419

40. Pietras EM, Reynaud D, Kang YA, Carlin D, Calero-Nieto FJ, Leavitt AD, et al. Functionally distinct subsets of lineage-biased multipotent progenitors control blood production in normal and regenerative conditions. *Cell Stem Cell* (2015) 17(1):35–46. doi: 10.1016/j.stem.2015.05.003

41. Chen ELY, Thompson PK, Zúñiga-Pflücker JC. RBP J-dependent Notch signaling initiates the T cell program in a subset of thymus-seeding progenitors. *Nat Immunol* (2019) 20(11):1456–68. doi: 10.1038/s41590-019-0518-7

42. Stanley P, Kumar V, Tanwar A. Roles of Notch glycoslation in signaling. *FASEB J* (2021) 35(S1). doi: 10.1096/fasebj.2021.35.S1.00061

43. Matsumoto K, Luther KB, Haltiwanger RS. Diseases related to Notch glycosylation. *Mol Aspects Med* (2021) 79:100938. doi: 10.1016/j.mam.2020.100938

44. Schröder KC, Duman D, Tekin M, Schanze D, Sukalo M, Meester J, et al. Adams–Oliver syndrome caused by mutations of the EOGT gene. *Am J Med Genet Part A* (2019) 179(11):2246–51. doi: 10.1002/ajmg.a.61313

45. Atzmony L, Zaki TD, Antaya RJ, Choate KA. Phenotypic expansion of POFUT1 loss of function mutations in a disorder featuring segmental dyspigmentation with eczematous and folliculo-centric lesions. *Am J Med Genet A* (2019) 179(12):2469–73. doi: 10.1002/ajmg.a.61362

46. Hozumi K, Mailhos C, Negishi N, Hirano K-I, Yahata T, Ando K, et al. Delta-like 4 is indispensable in thymic environment specific for T cell development. *J Exp Med* (2008) 205(11):2507–13. doi: 10.1084/jem.20080134

47. Stanley P, Guidos CJ. Regulation of Notch signaling during T- and B-cell development by O-fucose glycans. *Immunol Rev* (2009) 230(1):201–15. doi: 10.1111/j.1600-065x.2009.00791.x

48. Lakhan R, Rathinam CV. Deficiency of rbpj leads to defective stress-induced hematopoietic stem cell functions and hif mediated activation of non-canonical Notch signaling pathways. *Front Cell Dev Biol* (2021) 8:622190(1923). doi: 10.3389/fcell.2020.622190

49. Stanley P, Tanwar A. Regulation of myeloid and lymphoid cell development by O-glycans on Notch. *Front Mol Biosci* (2022) 9:979724(979724). doi: 10.3389/fmolb.2022.979724

50. Matsumoto K, Kumar V, Varshney S, Nairn AV, Ito A, Pennarubia F, et al. Fringe GlcNAc-transferases differentially extend O-fucose on endogenous NOTCH1 in mouse activated T cells. *J Biol Chem* (2022) 298:102064. doi: 10.1016/j.jbc.2022.102064

51. Wang W, Ozdemir V. Special issue: glycomics and personalized glycomedicine. *OMICS* (2019) 23(12):599–600. doi: 10.1089/omi.2019.0177